Embedded System for Detecting Underwater Ultrasound

Valeriya Naycheva[1], Lubomir Bogdanov[1] and Nikolay Iliev[2]
1) Department of Electronics, Faculty of Electronic Engineering and Technologies
Technical University of Sofia
8 Kliment Ohridski blvd., 1000 Sofia, Bulgaria
{vnaycheva, lbogdanov}@tu-sofia.bg

2)Nextlab Ltd
8 Kliment Ohridski blvd., 1000 Sofia, Bulgaria
nik@nlab.bg

Abstract – **The current paper focuses on the implementation details of a device that detects ultrasound at a distance of 1 m in sea water. This detector could be used to test the operation of ultrasonic emitting devices, called pingers, which deter cetacean mammals from entering fish nets of fishing boats at sea. The device is battery-powered and a low-energy Bluetooth connection is available for turning it on and off.**

Keywords – **Bluetooth connection; embedded system; low power; ultrasound detection; underwater sound.**

I. Introduction

Underwater mammals like dolphins, whales and porpoises tend to be tearing fishermen's nets when hunting for fish. Unfortunately this sometimes leads to the death of the mammal as it is entangled in the net's rope. This process is known as a bycatch [1], [2]. To protect those mammals, as well as their fishing nets, fishermen use underwater sound emitting devices called pingers. The sound frequencies for whales and porpoises are 3 kHz and 10 kHz respectively, and for dolphins – it is ≥ 60 kHz. The first two ranges can be heard by humans easily, as the frequency response of the human ear is 20 – 20000 Hz. The fisherman can test the operation status of those pingers by activating them in air. However, the third range is in the ultrasonic spectrum and cannot be heard without any additional equipment.

To cope with this problem, a device that is submerged in water and placed in close proximity to the pinger could detect the ultrasound with a specially-built for the purpose hydrophone. The proposed circuit activates an LED whenever there is ultrasound present nearby. This way the user will know, with a high level of certainty, that the pinger is working and that the nets can be immersed in water safely.

An example usage is shown in Fig. 1. At the deck, when the fishing net starts submerging, the pinger detector is activated with a smart phone through a Bluetooth interface. At this point, the analog part is powered on and the detection process is started. Whenever an ultrasound reaches the hydrophone, the signal is amplified and fed to an analog comparator. The output of this comparator is connected to a Bluetooth controller that transforms any toggling activity into light by an LED indicator. Usually the emitted sound by the pinger has a period of 50 – 300 ms which is enough to be seen by the human eye.

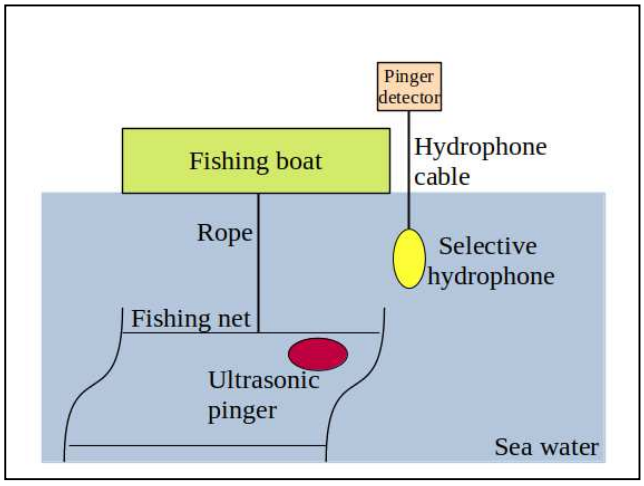

Fig. 1. Usage of the proposed ultrasonic detector.

Individual pingers could be tested the same way on deck with a basin of water which would guarantee that the distance between the pinger and the detector remains low (within 1 m). This method is the preferred one because submerging multiple pingers would activate the device constantly and the user would not know at any specific time which pinger is emitting the sound.

II. Block Diagram of the Detector

Fig. 2 shows the block diagram of the proposed hardware. The detecting device is a piezo buzzer used as a microphone/hydrophone. A thorough coverage on the operation and exploitation of underwater transducers is given in [3]. The piezo element need not be linear at all – it will detect frequencies in the range 60 – 80 kHz and therefore the same piezo that is used as an emitter can be used as a reception sensor that outputs a signal [4].

978-1-6654-9878-4/22/$31.00 ©2022 IEEE

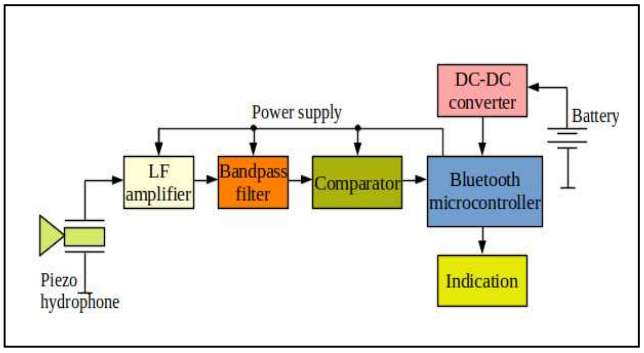

Fig. 2. Block diagram of the ultrasonic detector's hardware.

To extract the signal from the piezo with high accuracy and no losses, the input impedance of the amplifier must be high. This amplifier must be a low frequency one with a bandwidth of up to 80 – 100 kHz.

A band-pass filter is required to cut off sounds outside the required range. It is the main block in the analog front end. Sounds with lower frequencies, generated by human speech and naval boat engines, must not be amplified as this would result in false triggering of the detector. Sounds with higher frequencies also present a problem – e.g. ultrasound from sonar devices.

At the output of the band-pass filter a comparator is required to convert the analog signal into a digital one. If the microcontroller has one integrated on chip, this block is not necessary. Otherwise, the output of the comparator is connected to the GPIO port of the microcontroller.

The chosen microcontroller for this implementation is a Nordic Semiconductors' Bluetooth chip from the NRF52 family. Its sole purpose is to turn on and off the analog part, detect signal transitions on a GPIO (using interrupts) and activate another GPIO to turn on an LED indicator (designated as "indication" on the block diagram). This task can be accomplished with any other microcontroller, as long as it is a low-power one and a method to activate the device is available.

Finally, a high-efficiency DC-DC converter is needed to supply the circuit. The device is required to operate with a single C battery with rated voltage of 1.5 V. The DC-DC must be a step-up converter and its quiescent current must be as low as possible. In fact, it was measured that the main contributor to the power consumption in IDLE state is this block.

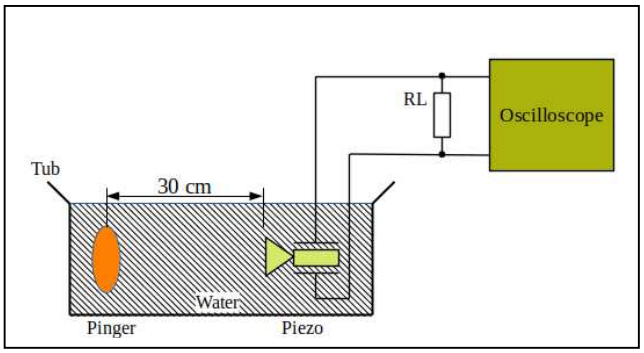

Fig. 3. The test setup for a piezo hydrophone measurements.

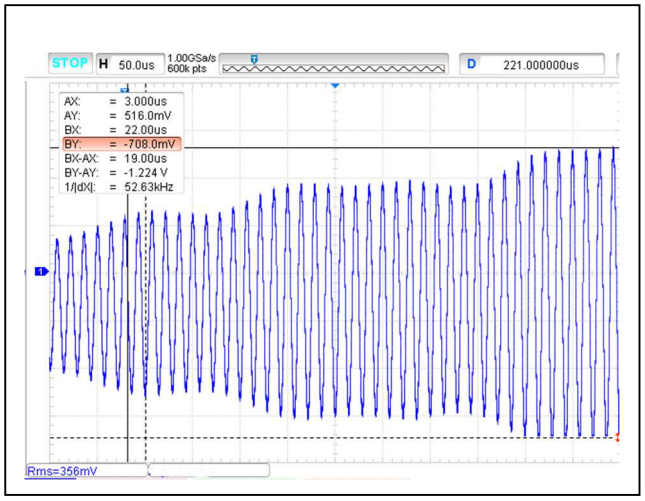

Fig. 4. Piezo hydrophone output at exposure to a 175 dB, 70-kilohertz pinger.

III. Hardware of the Analog Front End

An example circuit for connecting a piezo element to an RMS-to-DC converter is presented in [5]. This circuit could be used to directly measure the amplitude of the input signal. However, in the current paper the focus is to only detect the duration of the signal and display it with an LED.

The first step is to measure the output voltages of the piezo element at different loads and with different pinger types. The test setup is shown in Fig. 3 and the results are averaged, and shown in Table 1. The hydrophone is exposed to two types of pingers – a low- (145 dB SPL) and a high-power (175 dB SPL) pinger. The minimum detected amplitude was 58 mVp-p and the maximum – 1200 mVp-p.

Because in a real life situation the distance between the detector and the pinger may vary, as well as the tolerance of the components, the amplification of the circuit was increased from the theoretical Au = 57 to a more practical value Au = 100.

The input amplifier circuit is shown in Fig. 5. It is a classical implementation of an AC non-inverting amplifier with a single supply [6]. To avoid dual supplies, all of the analog circuits are designed to operate at VDD / 2. Level shifting of the input signal is accomplished with resistors R1 and R2, and C2 decouples the piezo sensor from the DC offset. The chosen amplification is Au = 10. The power supply 3V3 is provided by a GPIO pin of the microcontroller.

Table 1. Piezo Hydrophone Output Voltage (Average)

Resistive load	Piezo output with low power pinger, mVp-p	Piezo output with high power pinger, mVp-p
100 kΩ	95	571
4.7 MΩ	128	850
10 MΩ	146	706
∞	129	872

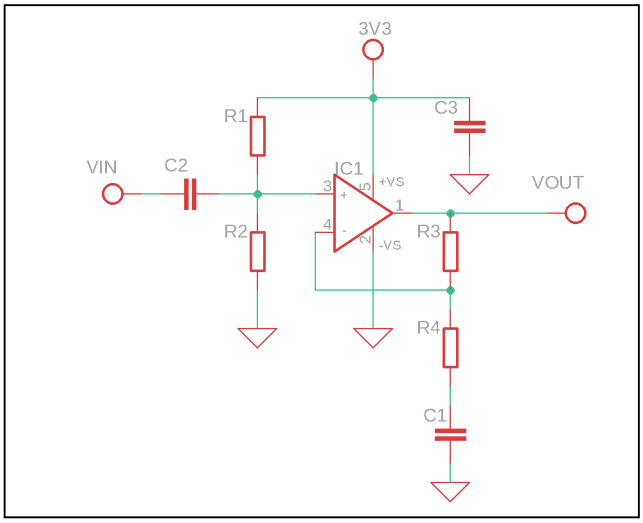

Fig. 5. Input amplifier stage of the ultrasonic detector.

The band-pass filter circuit is shown in Fig. 6. It is a multi-loop feedback (MLF), 2nd order filter circuit [7], [8]. This active filter was designed with an amplification value of Au = 10 and a center frequency f_0 = 70 kHz. Its frequency response is not steep, and the passive components were chosen to be the nearest 5-percent values, so deviation from the center frequency is expected. This way the price of the device would remain low. Resistors R8 and R9 are needed to supply a reference voltage of the circuit (VDD/2), because the pervious stage (the amplifier) has a DC-offset at its output.

The final block of the analog circuit is the optional comparator shown in Fig. 7. Microcontrollers with an integrated comparator need not have an external one. The circuit is built without any hysteresis. The resistors R10 and R11 apply a reference voltage at the inverting input of the operational amplifier. Its value is chosen in such a way that it is slightly above the VDD/2 offset. This ensures that signals with low amplitudes will not be passed to the controller. The latter ensures the noise immunity of the device.

A prototype board was built to measure the frequency response of the amplifier and the band-pass filter. The results are shown in Fig. 8. The first notable and expected problem is the shift of the center frequency from 70 kHz to 56 kHz.

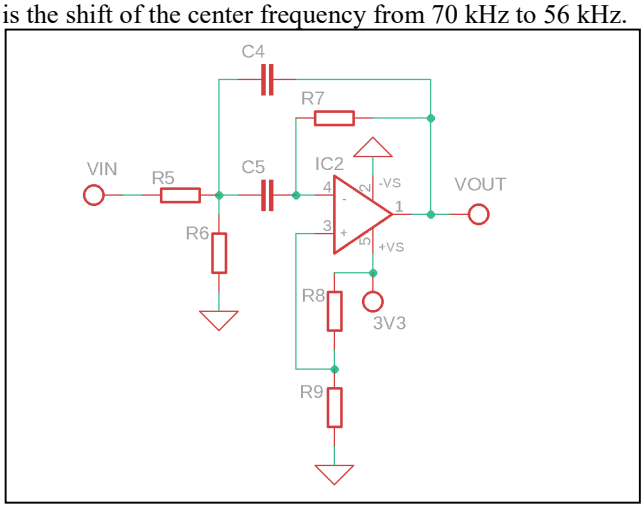

Fig. 6. The band-pass filter of the ultrasonic detector. This is the core of the analog front end.

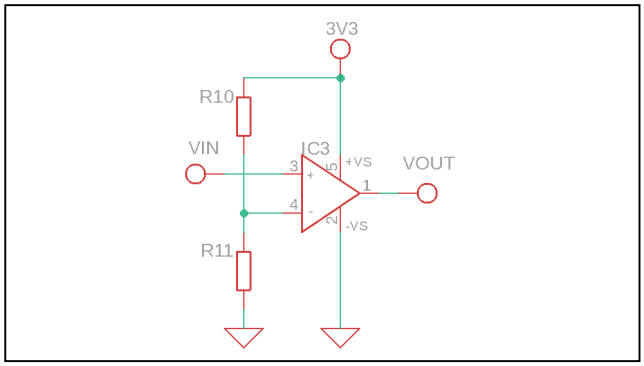

Fig. 7. The comparator circuit of the ultrasonic detector. This circuit is optional.

The second problem is the gain of the amplifier at 70 kHz – Au = 8.6 (instead of the theoretical 10). At 70 kHz, the combined gain is Au = 43. This value is accepted because using op-amps with higher GBWP and passive components with small tolerances would significantly increase the price of the device.

III. Software of the Digital Back End

As mentioned before, the Bluetooth connectivity allows for a low-power control of the device. It is implemented as a Bluetooth peripheral device. The firmware of the microcontroller is accepting connections from a smart phone and is executing SCPI commands issued by the user. Table 2 lists the currently supported commands and their function.

An algorithm of the firmware's main loop, as well as the GPIO interrupt handler, is shown in Fig. 9. Most of the time the microcontroller spends in a sleep mode. The sleep mode keeps an RTC timer on and the Bluetooth advertising active (waiting for connection). The RTC wakes the device up each second and checks whether there is a command from the user. A command will arrive only if a Bluetooth central device (such as a smart phone) is connected and a command has been issued.

If a command "ON" has been received, the microcontroller will assert its respective GPIO pin to power on the analog front end.

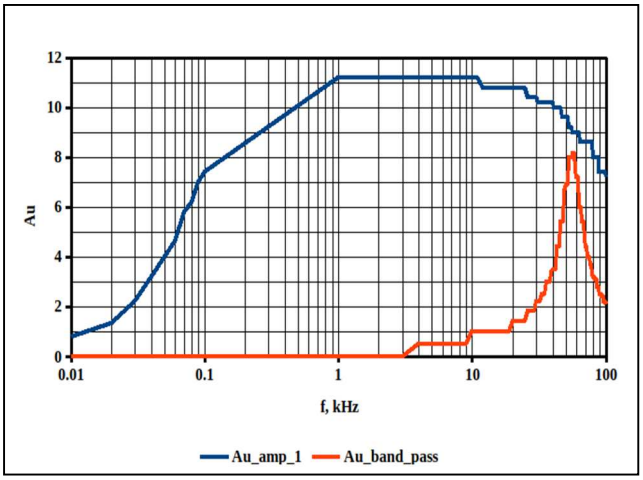

Fig. 8. Measured frequency response of the amplifier and the 2nd order band-pass filter.

TABLE 2. SUPPORTED SCPI COMMANDS OF THE BLUETOOTH INTERFACE

Command string	Function
*IDN?	Return device name, firmware and software revision.
HELP	Return a list with all of the supported commands.
ON	Exit IDLE mode and start detecting ultrasound.
OFF	Stop detecting ultrasound and enter IDLE mode.

The sourcing capability of NRF52's pins is up to 25 mA which is more than enough for the current application. All three op-amps can be powered by a single pin. Whenever an ultrasound is detected, the output of the comparator will start toggling the GPIO pin of the microcontroller. The microcontroller will service an interrupt, attached to this specific pin, and will set or clear the respective GPIO pin, connected to the LED indicator (green). A second LED indicator (yellow) will blink each second to inform the user that the detector is active.

If a command "OFF" has been received, the microcontroller will de-assert the GPIO to power off the analog front end. This will prevent further interrupts and the device will spend most of the time in sleep mode.

The Bluetooth stack has been built with the option for over-the-air updates (OTA, more information can be found in [9]). This helps in adding new features of the firmware, as well as clearing existing bugs. A typical 128 kB-firmware can be updated for less than 10 seconds with Nordic's application specifically built for the purpose. The only thing that has to be done in production, prior to shipping, is to flash with an SWD debugger not only the user firmware, but also the bootloader that will enable the OTA.

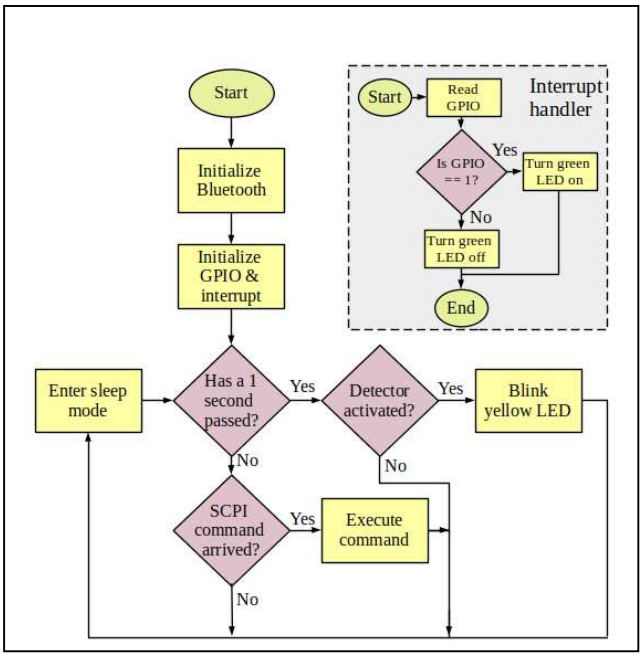

Fig. 9. Algorithm of the microcontroller's firmware.

TABLE 3. ENERGY CONSUMPTION OF THE DIFFERENT OPERATING MODES

Operating mode	Average current consumption, mA
IDLE	0,209
Central connected	0,775
Detecting ultrasound	5,100
Detecting and indicating with the green LED	14,900

IV. EXPERIMENTAL RESULTS

A complete prototype has been assembled and tested. The device operates as expected. Ambient noise in air, such as human speech and sounds, does not false-trigger the device. When immersed in water, the device successfully detects pingers at ranges of about 1 m. Both low- and high-power pingers are detected. The Bluetooth connection operates as expected. Energy consumption measurements are given in Table 3. The major contributors to the consumption during detection are the LEDs, as shown in Fig. 10. They are selected to be bright and are supplied with high currents to allow for noticeable indication during outdoor usage. The yellow LED is lit for a short amount of time to display that the detection is ongoing. The green LED is lit for up to 300 ms because it corresponds to the period of the detected sound. The small spikes in between are due to the Bluetooth radio that is advertising and waiting for connections. The Bluetooth alone consumes approximately 40 µA and if better current consumption is required, the optimization should aim at the LEDs and the quiescent current of the operational amplifiers.

V. CONCLUSION

An embedded device for detecting ultrasound emission underwater has been presented in this paper. Details of the hardware and the firmware are included. A prototype of the detector has been assembled and tested. Frequency response and energy consumption has been measured. All parameters are acceptable and the development can further add features to expand the capabilities of such a device.

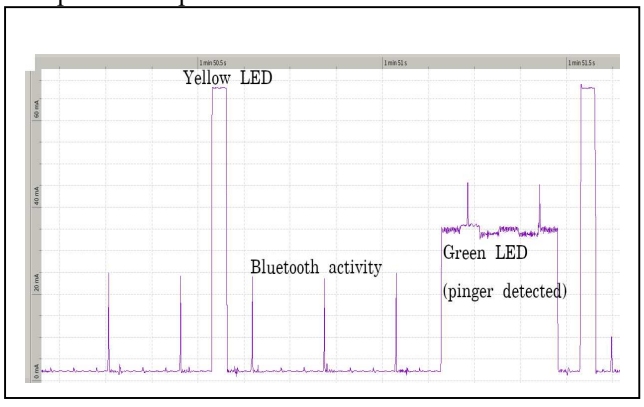

Fig. 10. Current consumption during detection.

Future improvements may include the addition of precision passive components for the filter, replacement of the step-up DC-DC converter with a more energy-efficient one to reduce the IDLE current, replacement of the LEDs with brighter but more low-power ones. If the price is of no concern, an additional peak detector could be added and its output could be connected to an ADC input. This would allow for amplitude measurement of the detected signal.

From software point of view, a feedback from the device could be provided, e.g. whenever a sound has been detected, the firmware may inform the application about this event. This gives the opportunity to create a virtual panel of the device running on a smart phone.

ACKNOWLEDGMENT

The authors would like to thank the Research and Development Sector at the Technical University of Sofia for the financial support.

REFERENCES

[1] C. Guidino, E. Campbell, A. Bielli, A. Pasara-Polack, J. Alfaro-Shigueto, J. Mangel, "Pingers Reduce Small Cetacean Bycatch in a Peruvian Small-Scale Driftnet Fishery, but Humpback Whale (Megaptera novaeangliae) Interactions Abound", Aquatic Mammals 48(2), pp.117-125, DOI: 10.1578/AM.48.2.2022.117, 2022.

[2] S. Dawson, E. Slooten, A. Read, "Pingers, porpoises and power: Uncertainties with using pingers to reduce bycatch of small cetaceans", Biological Conservation, DOI: 10.1016/S0006-3207(97)00127-4, 1998.

[3] C. Sherman, J. Butler, "Transducers and Arrays for Underwater Sound", Springer Science+Business Media LLC, ISBN-13: 978-0387-32940-6, 2007.

[4] M. Aleksandrova, "Piezoelectric Alternative Energy Sources As A Part Of The Global Energy Concerns – Future Prospects In The Science And Market", Advanced Materials Letters, 2020.

[5] I. Pandiev, M. Aleksandrova, "Design and Implementation of Dynamic FPAA Based Interface Circuit for Thin Film Lead-Free Piezoelectric Sensors", Advanced Materials Letters, 2020.

[6] "Analog Engineer's Circuit: Amplifier", SB0A224A, online, Texas Instruments, 2019.

[7] I. Pandiev, "Analog Circuits", in Bulgarian, Technical Univeristy of Sofia, ISBN: 978-619-167-195-3, 2015.

[8] "MC3403 Low Power Quad Bipolar Operational Amplifiers", ST Microelectronics, datasheet, 2001.

[9] A. Ahmed, S. Sharf, L. Said, A. Madian, "Design of IoT Microchip AVR Programmer for FOTA Updates based on Unified Programming and Debug Interface using Wi-Fi and LoRa", 28th IEEE International Conference on Electronics, Circuits, and Systems (ICECS), DOI: 10.1109/ICECS53924.2021.9665524, 2021.